Research Article | Vol. 26, No. 7 | 2 Apr 2018 | OPTICS EXPRESS 9155
Optics EXPRESS

Leaky mode integrated optical fibre refractometer

ALAN C. GRAY,* ALEXANDER JANTZEN, PAUL C. GOW, DEVIN H. SMITH, CORIN B. E. GAWITH, PETER G. R. SMITH, AND CHRISTOPHER HOLMES

Optoelectronics Research Centre, University of Southampton
*A.C.Gray@soton.ac.uk

Abstract: A route to monitor external refractive indices greater than the core index of the waveguide is presented. Initial application utilizes an integrated optical fibre (IOF) platform due to its potential for use in harsh environment sensing. IOF is fabricated using a bespoke flame hydrolysis deposition process to fuse an optical fibre to a planar substrate achieving an optical quality, ruggedized glass layer between the fibre and substrate was fabricated. The presented refractometer is created by direct UV writing of multiple fibre Bragg gratings into an etched (22 μm diameter) optical fibre post fabrication. Linear regression analysis is applied to quantify propagation loss by monitoring each FBG's back reflected power. The device operates with a sensitivity of approximately 350 dB/cm/RIU at a refractive index of 1.451 at 1550 nm. Numerical simulations using a transfer matrix method are presented and potential routes for development are discussed.

OCIS codes: (280.4788) Optical sensing and sensors; (060.3735) Fiber Bragg gratings; (130.0130) Integrated optics.

References and links

1. Q. Wang and G. Farrell, "All-fiber multimode-interference-based refractometer sensor: proposal and design," Opt. Lett. **31**(3), 317–319 (2006).
2. G. J. Veldhuis, L. E. W. van der Veen, and P. V. Lambeck, "Integrated optical refractometer based on waveguide bend loss," J. Lightwave Technol. **17**(5), 857–864 (1999).
3. W. Liang, Y. Huang, Y. Xu, R. K. Lee, and A. Yariv, "Highly sensitive fiber Bragg grating refractive index sensors," Appl. Phys. Lett. **86**(15), 151122 (2005).
4. C. Gouveia, P. A. S. Jorge, J. M. Baptista, and O. Frazao, "Fabry-perot cavity based on a high-birefringent fiber Bragg grating for refractive index and temperature measurement," IEEE Sensors J. **12**(1), 17–21 (2012).
5. K. R. Daly, C. Holmes, J. C. Gates, P. G. R. Smith, and G. D'Alessandro, "Complete mode structure analysis of tilted Bragg grating refractometers in planar waveguides toward absolute index measurement," IEEE Photon. J. **3**(5), 861–8871 (2011).
6. J. Albert, L.-Y. Shao, and C. Caucheteur, "Tilted fiber Bragg grating sensors," Laser Photon Rev. **7**(1), 83–108 (2013).
7. X. Shu, L. Zhang, and I. Bennion, "Sensitivity characteristics of long-period fiber gratings," J. Lightwave Technol. **20**(2), 255 (2002).
8. F. Shen, C. Wang, Z. Sun, K. Zhou, L. Zhang, and X. Shu, "Small-period long-period fiber grating with improved refractive index sensitivity and dual-parameter sensing ability," Opt. Lett. **42**(2), 199–202 (2017).
9. P. Chen, X. Shu, H. Cao, and K. Sugden, "Ultra-sensitive refractive index sensor based on an extremely simple femtosecond-laser-induced structure," Opt. Lett. **42**(6), 1157–1160 (2017).
10. M. Konstantaki, P. Childs, M. Sozzi, and S. Pissadakis, "Relief Bragg reflectors inscribed on the capillary walls of solid-core photonic crystal fibers," Laser Photon Rev. **7**(3), 439–443 (2013).
11. H. W. Yarranton, J. C. Okafor, D. P. Ortiz, and F. G. A. van den Berg, "Density and refractive index of petroleum, cuts, and mixtures," Energy Fuels **29**(9), 5723–5736 (2015).
12. A. Iadicicco, A. Cusano, A. Cutolo, R. Bernini, and M. Giordano, "Thinned fiber Bragg gratings as high sensitivity refractive index sensor," IEEE Photon. Technol. Lett. **16**(4), 1149–1151 (2004).
13. K. Schroeder, W. Ecke, R. Mueller, R. Willsch, and A. Andreev, "A fibre Bragg grating refractometer," Meas. Sci. Technol. **12**(7), 757 (2001).
14. Y. Jung, S. Kim, D. Lee, and K. Oh, "Compact three segmented multimode fibre modal interferometer for high sensitivity refractive-index measurement," Meas. Sci. Technol. **17**(5), 1129 (2006).

#318100 https://doi.org/10.1364/OE.26.009155
Journal © 2018 Received 21 Dec 2017; revised 16 Feb 2018; accepted 2 Mar 2018; published 29 Mar 2018

Optics EXPRESS

15. X. Zhang and W. Peng, "Fiber optic refractometer based on leaky-mode interference of bent fiber," IEEE Photon. Technol. Lett. **27**(1), 11–14 (2015).
16. I. Sparrow, G. Emmerson, C. B. E. Gawith, and P. G. R. Smith, "Planar waveguide hygrometer and state sensor demonstrating supercooled water recognition," Sens. Actuat. B **107**(2), 856 – 860 (2005).
17. C. Holmes, A. Jantzen, A. C. Gray, P. C. Gow, L. G. Carpenter, R. H. S. Bannerman, J. C. Gates, and P. G. R. Smith, "Evanescent field refractometry in planar optical fiber," Opt. Lett. **43**(4), 791–794 (2018).
18. C. Holmes, J. C. Gates, L. G. Carpenter, H. L. Rogers, R. M. Parker, P. A. Cooper, S. Chaotan, F. R. M. Adikan, C. B. E. Gawith, and P. G. R. Smith, "Direct UV-written planar Bragg grating sensors," Meas. Sci. Technol. **26**(11), 112001 (2015).
19. C. Holmes, P. A. Cooper, H. N. J. Fernando, A. Stroll, J. C. Gates, C. Krishnan, R. Haynes, P. L. Mennea, L. G. Carpenter, C. B. E. Gawith, M. M. Roth, M. D. Charlton, and P. G. R. Smith, "Direct UV written planar Bragg gratings that feature zero fluence induced birefringence," Meas. Sci. Technol. **26**(12), 125006 (2015).
20. C. Sima, J. C. Gates, H. L. Rogers, P. L. Mennea, C. Holmes, M. N. Zervas, and P. G. R. Smith, "Ultra-wide detuning planar Bragg grating fabrication technique based on direct UV grating writing with electro-optic phase modulation," Opt. Express **21**(13), 15747–15754 (2013).
21. H. L. Rogers, S. Ambran, C. Holmes, P. G. R. Smith, and J. C. Gates, "In situ loss measurement of direct UV-written waveguides using integrated Bragg gratings," Opt. Lett. **35**(17), 2849–2851 (2010).
22. F. Grillot, L. Vivien, S. Laval, D. Pascal, and E. Cassan, "Size influence on the propagation loss induced by sidewall roughness in ultrasmall soi waveguides," IEEE Photon. Technol. Lett. **16**(7), 1661–1663 (2004).
23. S. Selleri, L. Vincetti, A. Cucinotta, and M. Zoboli, "Complex FEM modal solver of optical waveguides with PML boundary conditions," Opt. Quantum Electron. **33**(4), 359–371 (2001).
24. H. P. Uranus and H. Hoekstra, "Modelling of microstructured waveguides using a finite-element-based vectorial mode solver with transparent boundary conditions," Opt. Express **12**(12), 2795–2809 (2004).
25. G. B. Hocker and W. K. Burns, "Mode dispersion in diffused channel waveguides by the effective index method," Appl. Opt. **16**(1), 113–118 (1977).
26. L. C. Andreani and D. Gerace, "Photonic-crystal slabs with a triangular lattice of triangular holes investigated using a guided-mode expansion method," Phys. Rev. B **73**(23), 235114 (2006).
27. W. P. Huang and C. L. Xu, "Simulation of three-dimensional optical waveguides by a full-vector beam propagation method," IEEE J. Quantum Electron. **29**(10), 2639–2649 (1993).
28. K. Saitoh and M. Koshiba, "Full-vectorial finite element beam propagation method with perfectly matched layers for anisotropic optical waveguides," J. Lightwave Technol. **19**(3), 405 (2001).
29. A. Ghatak, K. Thyagarajan, and M. Shenoy, "Numerical analysis of planar optical waveguides using matrix approach," J. Lightwave Technol. **5**(5), 660–667 (1987).
30. M. R. Ramadas, A. K. Ghatak, K. Thyagarajan, E. Garmire, and M. R. Shenoy, "Analysis of absorbing and leaky planar waveguides: a novel method," Opt. Lett. **14**(7), 376–378 (1989).
31. J. Pendry, "Photonic band structures," J. Mod. Opt. **41**(2), 209–229 (1994).
32. L. L. Lin, Z. Y. Li, and K. M. Ho, "Lattice symmetry applied in transfer-matrix methods for photonic crystals," J. Appl. Phys. **94**(2), 811–821 (2003).
33. P. Bienstman, S. Selleri, L. Rosa, H. P. Uranus, W. C. L. Hopman, R. Costa, A. Melloni, L. C. Andreani, J. P. Hugonin, P. Lalanne, D. Pinto, S. S. A. Obayya, M. Dems, and K. Panajotov, "Modelling leaky photonic wires: A mode solver comparison," Opt. Quantum Electron. **38**(9), 731–759 (2006).
34. B. Hooda and V. Rastogi, "Low cost highly sensitive miniaturized refractive index sensor based on planar waveguide," Optik Int. J. Light. Electron. Opt. **143**, 158 – 166 (2017).

1. Introduction

As optical devices are not subject to interference from external electromagnetic fields, they have been of great interest in recent decades for use in sensing technologies. In the field of refractometry, a number of techniques have been proposed: optical fibre-based multi-mode interference [1], bend loss [2], fibre Bragg gratings (FBG) [3,4], tilted Bragg gratings [5,6], long-period FBGs [7,8], optical fibre Fabry-Perot interferometers [9] and relief Bragg reflectors [10]. The additional advantage of using silica based devices is their chemical inertness. FBGs may be used as sensors in several configurations: Wet-etched, D-shaped, microstructured and side-polished optical fibre all present methods of chemical or biological sensing via interrogation of an FBG's response to the surrounding-medium refractive index (SRI).

Typically the response characterized is a shift in the Bragg wavelength, which is a function of the waveguide's effective index and is exponentially responsive as the SRI increases towards the core's refractive index. As the refractive index of many hydrocarbons is slightly above that of silica, such as alkylaromatics found in jet fuels and diesel [11], development of a technique

Optics EXPRESS

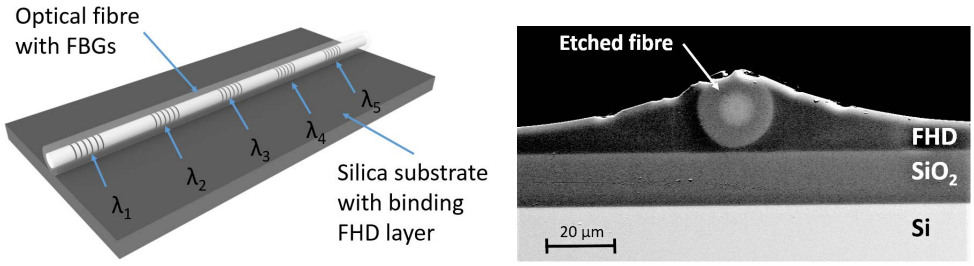

(a) (b)

Fig. 1. (a) Schematic of the integrated optical fibre refractometer. Each λ corresponds to a different period FBG wrote into the etched optical fibre via direct UV grating writing. (b) Backscatter scanning electron micrograph of the end facet of the presented refractometer.

which allows for refractometry above the index of the sensor is required. Silica devices such as thinned-FBGs [12] and side-polished FBGs [13] both enable refractometry for indices below that of silica. Leaky mode waveguides are an alternative refractometry platform due to the mode confinement being dependent on the SRI [14, 15]. The presented refractometer operates as a leaky waveguide in which propagation loss measurements are used to quantify the device's response to the SRI. Propagation loss in this device is characterized by FBGs which are direct UV written into the fibre in the final stages of fabrication, combining the advantages of leaky mode and FBG devices.

Integrated optical fibre (IOF) is a novel platform in which an optical fibre is bound to a silica-on-silicon substrate. This is achieved through a modified flame hydrolysis deposition (FHD) technique which forms an optical quality glass between the fibre and substrate. IOF enables the optical qualities of fibre to be combined with the mechanical strength of a planar substrate. Thinned FBGs have been shown to have a 10^{-5} refractive index resolution but the fragility of the fibre post-etching was a limitation in the application of such a device [12]. State of the art refractometers have a resolution approaching 10^{-6} [16] which is the goal for any new refractometry device. The IOF platform has the potential to overcome the issue of fragility in etched optical fibre refractometers. The presented refractometer is shown to be responsive to refractive indices greater than that of the fibre core. Although the IOF platform was selected for this work, the presented methodology has the potential to be applied to any optical waveguiding platform of which the refractive index of the material is below that of the analyte. This work builds on a previously demonstrated IOF refractometer which was based on thinned FBGs for evanescent field sensing [17] and was characterised by means of a shift in Bragg wavelength. In this paper, initial results are presented along with a theoretical analysis of the device and means for improvement.

2. Fabrication

2.1. Flame hydrolysis deposition

SMF-28 fibre (Corning Inc.) was etched using a dilute hydrofluoric acid solution. Etching was terminated through neutralisation with deionised water when the fibre reached an approximate thickness of 25 µm. This was verified using a Nikon Eclipse LV100 polarising microscope. The etched optical fibre is bound to a silica substrate via FHD to form a ruggedized glass composite. The optical fibre was placed on a silicon substrate with a 15 µm thermal oxide top layer. The thick silica cladding layer ensures optical isolation of the propagating light in the fibre during experimentation, and thus that propagation loss is solely dependent on the analyte. FHD deposits a soot with an oxygen-hydrogen flame and precursors silicon tetrachloride, boron trichloride and

Optics EXPRESS

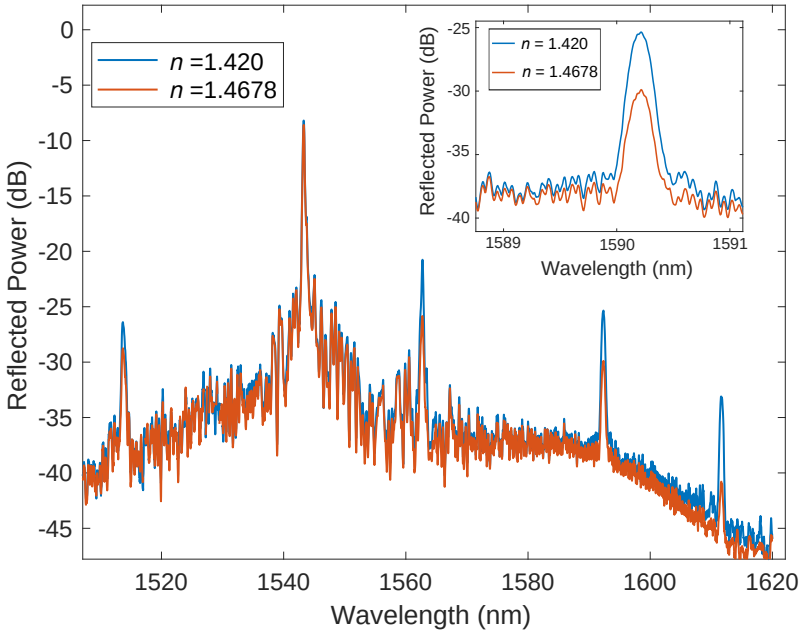

Fig. 2. Example of the back reflection spectrum of the device. One spectrum (n=1.42) is representative of indices lower than the device's effective index, the other spectrum (n=1.4678) displays a clear reduction in FBG-reflected power due to comparitively high propagation loss in the waveguide. A moving average method is applied to the spectra for ease of understanding the analysis technique. The λ_i labelling corresponds to those in Fig. 1(a). Inset displays a zoomed in graph of the reduction in FBG amplitude at approx. 1590 nm.

phosphorus trichloride. The soot is consolidated at 1100 °C. The consolidated FHD layer is optical-quality glass and has been used to create planar buried channel waveguide structures [18, 19]. The resulting wafer was diced to a 21 mm in length chip using a Loadpoint Microace precision dicing saw. The photosensitivity of the fibre core was enhanced by hydrogenation at 120 bar for 10 days prior to UV writing.

2.2. *Direct UV writing*

As UV light induces a refractive index change in photosensitive glass, direct UV grating writing (DUGW) enables a single-step process for writing multiple Bragg gratings of different period in planar waveguides or optical fibres. A 244 nm frequency-doubled CW argon-ion laser beam is split, focused and recombined at the focal point to create interference fringes in the waveguide core to create a Bragg grating. One of the paths of the beam passes through a computer controlled electro-optic modulator (EOM), enabling a rolling fringe pattern as the laser is translated along the fibre. The fibre is not assumed to to be perfectly straight. Therefore, a fourth order polynomial was fit to the fibre in the x-y plane thus that the focussed spot could translate through the fibre core during grating writing. Five 3 mm fibre Bragg gratings were written into this device at varying Bragg wavelengths. As a result of current alignment challenges of defining FBGs into the IOF through DUGW, only five FBGs were considered for this length of a device. Through improvement in UV laser alignment and grating strength, denser multiplexed gratings could be defined, which would be expected to reduce error in future work of this nature. The small spot size

Optics EXPRESS

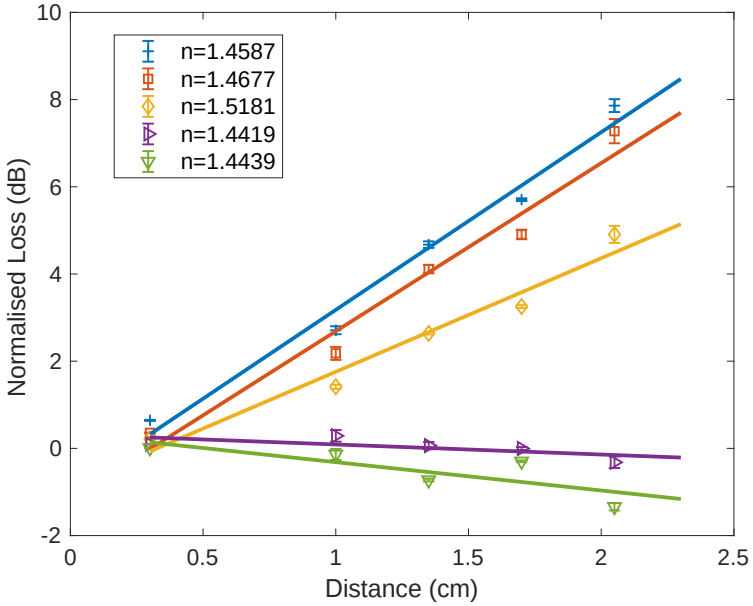

Fig. 3. An example data set of the power loss at each FBG in the refractometer along the device using the described method. The slope of the data is seen to be dependent on the analyte's refractive index.

(7 µm) used provides the means for a large Bragg wavelength tunability [20]. Hence, each FBG is a distinct wavelength and the location of each FBG is known during optical interrogation. The device is connected via a PM fibre V-groove pigtail with UV curing glue (Dymax OP-4-20632) prior to data collection.

3. Experimental and analytic methods

The device was interrogated with a superluminescent diode (Amonics ASLD-CWDM-5B-FA), and the reflection spectrum characterised using an optical spectrum analyzer (OSA) (ANDO AQ6317B). The reflected signal was obtained using a 3 dB coupler, example data set shown in Fig. 2. To alter the refractive index external to the device, calibrated refractive index oils were used (Cargille-Sacher Laboratories Inc., series A and AA). To determine a reference FBG amplitude for each respective grating, the device was covered in an oil of n=1.42. This index is below the effective index of the fibre and is assumed to maximise mode containment. It should be noted that all refractive indices recorded in this paper are scaled using the Cauchy equation considering wavelengths of 1550 nm from the calibrated value at 633 nm. Further measurements to calibrate this refractometer normalised the reference FBG amplitude to the measured spectrum. For each of the five FBGs, a data point is gathered per external refractive index value. An example of this data is displayed in Fig. 3. Loss at each grating position was normalised by the difference of the FBG's reflected power and the reference FBG amplitudes. The propagation loss is the gradient of a linear fit to each data set using the least-squares method. This method is a development and application of the propagation loss measurement technique proposed by Rogers *et al.* [21].

Spectral data was collected for each refractive index oil which were applied in a pseudorandom order to reduce the impact of remnant oil. Between data collection with different oils the device was cleaned using acetone and isopropyl alcohol, and dried with compressed air. The resulting data is shown in Fig. 4. Error bars displayed are representative of the standard error associated

Optics EXPRESS

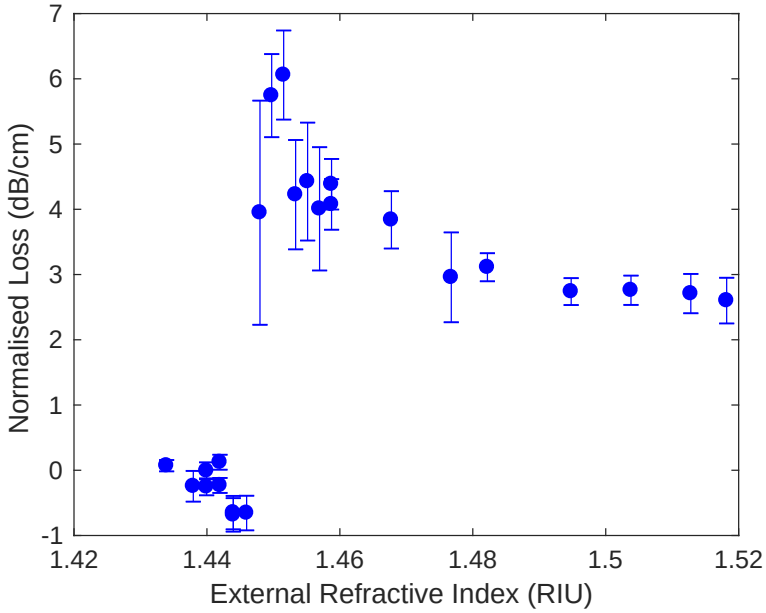

Fig. 4. External indices below that of the device's effective index are seen to be minimal in propagation loss and a distinct response curve for higher refractive indices.

with the slope of each linear fit to the corresponding data set. The comparatively large error for the data set at a refractive index of 1.448 is likely due to dispersion effects due to the wavelength difference between the FBGs used. This shall be addressed later in this paper. The negative propagation loss from 1.43-1.444 may be explained as a reduction in scattering loss at the fibre-analyte interface [22] as the external analyte approaches the effective index of the IOF waveguide. The effective index of the presented device is approximately 1.446. Current device sensitivity is 350 dB/cm/RIU at indices of 1.451.

4. Theoretical analysis

In the following section, we introduce a theoretical analysis of the proposed device to determine a route for further developments and a greater understanding of device limitations. A number of techniques have been developed for mode solving in optical waveguides. These techniques include finite element methods (FEM) [23, 24], the effective index method (EIM) [25], guided-mode expansion method [26], beam propagation method (BPM) [27,28] and the transfer matrix method (TMM) [29–32]. An extensive review and comparison of these techniques is presented by Bienstman *et al.* [33].

The technique used here is a modified TMM developed by Ramadas *et al.* [30] and was recently used in a similar leaky waveguide analysis [34]. This technique is explicitly applicable to planar waveguide structures in which the outer layers are semi-infinite. The method is relatively straightforward and allows the complex propagation constant, β_i, to be evaluated by real matrices, derived by considering electric field continuity at the interfaces. It should be noted that this is a one dimensional approximation of the presented device to affirm the trend of the data observed in Fig. 4, rather than a direct comparison of absolute propagation loss results with experimental values.

The following simulation results will be applied to the structure displayed in Fig. 5. For this

Optics EXPRESS

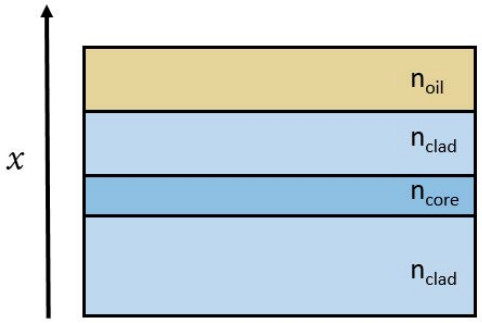

Fig. 5. A schematic of the model which is presented as part of this work. This simplification corresponds to a vertical slice of the IOF refractive index sensor solved for but may apply to any planar waveguide.

work, the refractive index of the core in SMF-28 is taken to be 1.45 with a diameter of 8.2 μm and the clad at $n = 1.444$. The FHD layer used in this device was a clad recipe which has a refractive index equal to the optical fibre clad and does not need to be considered as a separate layer in the model. An initial assumption is made that the electric field in the ith layer has the form

$$E_i = A_i \cos((x - d_i)k_i) + B_i \xi_i \sin((x - d_i)k_i), \tag{1}$$

where A_i and B_i are arbitrary constants, $k_i = (k_0^2 n_i^2 - \beta^2)^{1/2}$ and $\xi_i = 1/k_i$ for the TE polarisation case. x_i and d_i are the position within the layer and the location of the layer's boundary, respectively. The transfer matrix, g, representing the system is evaluated by

$$g := \prod_{n=i}^{1} S_i \tag{2}$$

where the transfer matrix for each individual layer, S_i is

$$S_i := \begin{cases} \begin{bmatrix} \cos(\Delta_i) & \xi_i \sin(\Delta_i) \\ -\frac{1}{\xi_i} \sin(\Delta_i) & \cos(\Delta_i) \end{bmatrix} & \text{for } k_i \in \mathbb{R} \\ \begin{bmatrix} \cosh(-i\Delta_i) & \gamma_i \sinh(-i\Delta_i) \\ \frac{1}{\gamma_i} \sinh(-i\Delta_i) & \cosh(-i\Delta_i) \end{bmatrix} & \text{for } k_i \in i\mathbb{R} \end{cases} \tag{3}$$

$\Delta_i = k_i(d_{i+1} - d_i)$ and $\gamma_i = i\xi_i$. The TE polarisation is the only case which shall be investigated in the progress of this work, as per the experimental data.

The waveguide, in its entirety, is defined as

$$\begin{bmatrix} A_C \\ B_C \end{bmatrix} = g \begin{bmatrix} A_1 \\ B_1 \end{bmatrix} \tag{4}$$

where A_1 and B_1 represent the electric field constants in the substrate and A_C and B_C correspond to the covering material. In this work, the cover is the analyte. Considering exponential decay of the electric fields in the outermost layers, Ramadas *et al.* assign the conditions $A_1 = \gamma_1 B_1$ and $A_C = -\gamma_C B_C$ to derive the eigenvalue equation

$$F(\beta) = \gamma_1 g_{11} + g_{12} + \gamma_C \gamma_1 g_{21} + \gamma_C g_{22} = 0. \tag{5}$$

As per Ramadas *et al.*'s technique, plotting $|1/F(\beta)|^2$ as a function of effective index, the half width at half maximum (HWHM) of the Lorentzian shaped resonance peak equates to the

Optics EXPRESS

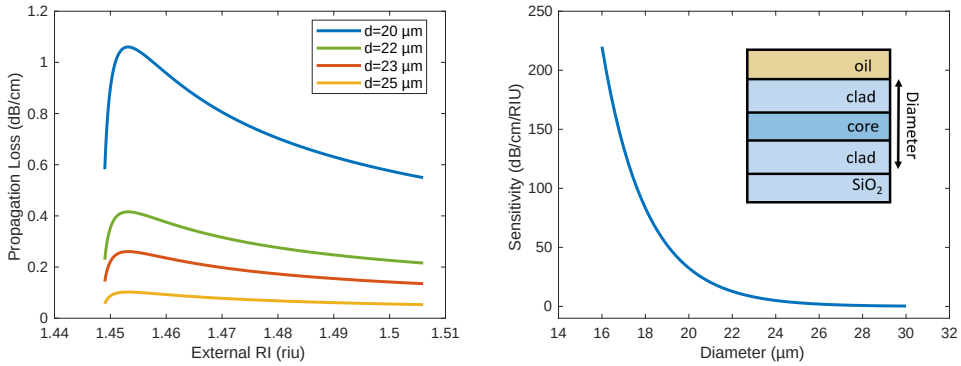

(a) (b)

Fig. 6. (a) Numerical simulation results of propagation loss for different fibre diameters. (b) Theoretical sensitivity of a planar model of the device at a refractive index of 1.456. An exponential increase in sensitivity is shown with respect to a decreasing diameter.

complex propagation constant, β_i. Hence, propagation loss as a function of the refractive index of the analyte can be extracted. In Fig. 6(a) the dependence of this structured device's propagation loss is shown for a set of different fibre diameters. This is equivalent to the diameter used for the experimental data shown in Fig. 4. In Fig. 6(a), a region with a high dependence on the analyte refractive index can be seen for each simulated data set. Therefore, this IOF refractive index sensor is most sensitive for applications in the range of 1.449–1.4525, while a broader but less-sensitive operating range exists for indices above 1.455, after the peak in propagation loss. The sensitivity of this device (dB/cm/RIU) is dependent on the etched fibre diameter used, as may be concluded from Fig. 6(a), and explicitly displayed in Fig. 6(b). A sensitivity greater than 200 dB/cm/RIU is calculated for a 16 µm diameter in comparison to approximately 15 dB/cm/RIU at 22 µm. With a core diameter of 8.2 µm, this equates to a 3.9 µm upper clad in the simulation. The lower limit of 16 µm for simulation was selected due to the limitations of fabrication. These include the non-trivial task of fabricating a straight IOF device as the fibre is increasingly susceptible to bending. It should also be noted, a device is limited by the reflecting power of the FBG. For example, a FBG that is 20 dB above the background level would not be measurable if it propagated through 2 cm of a 16 µm waveguide, using the parameter set in these simulations. Stronger gratings or an increased fibre diameter would be required.

It is also worth considering the effect of inherently lossy liquids on the propagation loss of a leaky waveguide such as that presented. Liquids with an extinction coefficient of the order of 10^{-6}, such as the aromatic hydrocarbon toluene, the model by Ramadas *et al.* predicts a change of the order 10^{-4} dB/cm for the device presented. As this is within the uncertainty in the regression analysis of the current device, it will not be considered further. However, if the analyte had an extinction coefficient of at least 2 orders of magnitude greater than this, this would be a limitation of leaky waveguide refractometry.

5. Discussion

The FBG linear regression analysis method for quantifying propagation loss in an optical waveguide may also be applied in a planar structure, such as those presented by Holmes *et al.* [18] if the upper clad is sufficiently thin. An advantage to the IOF platform for this application may be noted in the comparison to the theoretical work presented. For a fixed optical fibre diameter, 22 µm in this case, the experimentally determined maximum loss at a refractive index of 1.451 is

Optics EXPRESS

approximately 6 dB/cm. This compares to 0.415 dB/cm in the theoretical planar simulations for a 22 µm waveguide diameter displayed in Fig. 6(a). Another potential method for modification which is uniquely available to the IOF platform is the capability to decrease the FHD thickness and further expose the IOF to optical leakage in the horizontal plane on either side of the fibre. However, maximizing propagation loss in this manner may reduce the FBG back reflection power to within the noise of the spectrum. The TMM technique used in this work may be modified to account for the analyte on both sides of the waveguide, Fig. 5. This allows a simplification as γ_1 and γ_C in equation 5 are equivalent.The resulting maximum propagation loss for a double-sided planar device is calculated as approximately 0.83 dB/cm for an equivalent 22 µm fibre diameter. This provides a potential route for enhanced refractive index resolution or decreasing the length of the device, per the applications requirement.

The comparatively large error corresponding to the linear regression analysis of the $n = 1.448$ data in Fig. 4 is largely driven by two unaffected FBGs with respect to their back reflected power. This is potentially due to dispersion in which the respective FBG's wavelength is subjected to a different analyte refractive index. In this case, the lower wavelength FBGs were non-responsive. This is consistent with the theory, in which the analyte's refractive index must be greater than the effective index of the leaky mode waveguide. This effect may be reduced by UV writing FBGs of very similar wavelengths. This is easily achievable using the DUGW technique. Given this, if the uncertainty in calculated propagation loss in the presented device is reduced, refractive index resolution is expected to approach the order of 10^{-5} for a 0.01 dB/cm propagation loss resolution. This loss resolution is within the error found in the technique by Rogers *et. al* [21]. This method, which utilizes a bidirectional launch approach, has the benefit of inherent self-referencing rather than reference data being calibrated for a set index. However, However, this is difficult to implement for large values of loss when Bragg gratings completely disappear. Depending upon application, this technique can be implemented. Improvement in alignment to the IOF waveguide during DUGW to increase the strength of each Bragg grating without increasing the length is expected to reduce error in the regression analysis. Optimized conditions will be dependent upon specific application.

Due to the two possible solutions for refractive index for a given propagation loss, seen in Fig. 6(a), a reference refractometer could be used in conjunction to differentiate between the possible solutions. A reference refractometer may be realised in terms of a leaky planar waveguide with a different effective index to this device or an identical device with the core's refractive index altered through UV exposure. An additional justification for the use of FBGs in the presented refractometry technique is the dependence of Bragg wavelength on temperature. The Bragg wavelength shift due to the altering external refractive index was found to be negligible in this work. Hence, any Bragg wavelength shift could be accredited to temperature fluctuations.

6. Conclusion

A method for refractometry for refractive indices above that of the waveguide's core has been presented. An etched IOF refractometer was fabricated with multiple FBGs as the method of quantifying propagation loss in the leaky mode waveguide. This enabled calibration of the device's response to a liquid analyte's refractive index. The device has shown a potential refractive index resolution in the order of 10^{-5}. Results from an approximated TMM simulation have presented a number of routes for development of the device. This form of etched IOF presents itself as a candidate for harsh environment sensing due to its inherent chemical stability as a purely Si/SiO_2 sensor. Future work will include an investigation into optical fibre extruding from the substrate for optimal device coupling without the need for glues. This will further develop the device's application in harsh environments and as a method for reduced coupling losses.

Optics EXPRESS

Funding

Air Force Office of Scientific Research (FA9550-16-1-0531); Engineering and Physical Sciences Research Council (EPSRC) UK Quantum Technology Hub for Sensors and Metrology (EP/M013294/1); Higher Education Innovation Funding: University of Southampton Zepler Institute Research Collaboration Stimulus Fund (HEFCE).

Acknowledgments

The data for this work is accessible through the University of Southampton Institutional Research Repository (DOI https://doi.org/10.5258/SOTON/D0412).